New phases in antiferromagnetic spin-crossover chains

Carsten Timm[1, *] and Ulrich Schollwöck[2]

[1]*Institut für Theoretische Physik, Freie Universität Berlin, Arnimallee 14, D-14195 Berlin, Germany*
[2]*Institut für Theoretische Physik C, RWTH Aachen, D-52056 Aachen, Germany*
(Dated: October 25, 2004)

Spin-crossover molecules having a low-spin ground state and a low lying excited high-spin state are promising components for molecular electronics. We theoretically examine one-dimensional spin-crossover chain molecules. A prototypical compound is $[Fe^{2+}(R\text{-}trz)_3]_n$, where R-trz stands for 1,2,4-triazole with an organic side group R. The existence of the additional low-spin/high-spin degree of freedom leads, together with interactions, to rich physical behavior already in the ground state. We obtain the complete ground-state phase diagram, taking into account the elastic nearest-neighbor interaction, a ferromagnetic or antiferromagnetic exchange interaction between the magnetic ions, and an external magnetic field. The energies of various phases are calculated with high numerical precision using the density-matrix renormalization group (DMRG). Besides pure low-spin, high-spin, and alternating low-spin/high-spin phases we obtain a number of periodic ground states with longer periods, which we discuss in detail. For example, for antiferromagnetic coupling and small magnetic field there is a dimer phase with a magnetic unit cell containing two high-spin ions forming a spin singlet and a single low-spin ion, which is stabilized by the energy gain for singlet formation.

PACS numbers: 75.10.Jm, 75.50.Xx, 85.65.+h

I. INTRODUCTION

One of the most active fields of materials science to emerge in recent years is *molecular electronics*,[1,2] which proposes to use individual molecules as electronic components. A related idea is to use a single quantum spin, say of an ion, to store information, ideally with purely electronic read and write mechanisms. It has been emphasized by Kahn and coworkers[3,4,5] that *spin-crossover compounds*[6,7,8,9,10] (SCC's) are particularly promising for molecular memory devices.

These compounds consist of complexes involving transition metal ions and organic ligands.[7,8,9,10] The magnetic ions can be either in a low-spin (LS) or high-spin (HS) state, i.e., for the spin operator $\mathbf{S}_i$ at site i the eigenvalues of $\mathbf{S}_i \cdot \mathbf{S}_i$ are $S_{LS}(S_{LS} + 1)$ and $S_{HS}(S_{HS} + 1)$ in the LS and HS state, respectively. The energy difference between HS and LS states is due to the interplay between the crystal field splitting, which prefers doubly occupied d-orbitals and hence LS, and Hund's first rule, which favors unpaired spins and thus the HS state.[7,8,9,10] The term SCC is usually applied when the LS state is the ground state and the HS state is at a moderate (thermal) excitation energy. Often intermediate spin states also exist but are typically at much higher energies. SCC's show a characteristic crossover from the LS ground state to dominantly HS behavior at higher temperatures.[6] This is an entropic effect due to the higher degeneracy of the HS state. This crossover is typically sharper than expected for noninteracting magnetic ions and is even replaced by a first-order transition at a finite temperature in several compounds.[7,8,9,10]

Spin-crossover phenomena were first observed by Cambi and Szegö[6] in the 1930's. It has since been shown that SCC's can be switched back and forth between their states not only by changing the temperature but also by light, pressure, and an external magnetic field. The switching with light, known as *light-induced excited spin state trapping* (LIESST), has been demonstrated for the first time by Decurtins *et al.*[11] Spin-crossover phenomena are also observed in organic radicals[12] and certain inorganic transition-metal compounds.[13]

Of the large number of known SCC's some naturally form one-dimensional chains, for example Fe^{2+} with 4-R-1,2,4-triazole ligands.[4,14] Three ligands form bridges between two adjacent iron ions. Other SCC's consist of two-dimensional layers, e.g., $TlSr_2CoO_5$.[13,15] There is strong hope that many more one- and two-dimensional SCC's can be tailored by systematic variation of the ligand molecules.[16] It should be possible to have chains form in solution, which can subsequently be deposited onto a surface. Such one-dimensional SCC's appear to be the most promising candidates for technological applications, in particular in view of recent work on carbon nanotubes and DNA molecules.[17,18] Of course, SCC's add magnetism and the spin-crossover and LIESST effects, hopefully leading to interesting new phenomena and perhaps new functionalities.

On the other hand, SCC's are also very interesting from a statistical-physics point of view. In comparison to conventional local-moment systems they introduce an additional degree of freedom σ_i of Ising-type, which distinguishes between the LS ($\sigma_i = +1$) and HS ($\sigma_i = -1$) states. In the case of a *diamagnetic* LS state with spin $S_{LS} = 0$ the spins in the LS state are essentially switched off. These SCC's are thus related to site-diluted spin models,[19,20,21] but in our case the presence or absence of a spin is itself a *dynamical* variable and not a type of quenched disorder. Also related are recent studies of magnetic models with mobile vacancies,[22] which are motivated by cuprates with mobile defects, and of insulating phases of atoms with spin $S = 1$ in optical lattices.[23] As

we shall see, there is also a close relation to finite anti-ferromagnetic spin chains.

Antiferromagnetic spin chains came to the center stage of physical interest due to Haldane's (in the meantime firmly established) conjecture of a fundamental difference between (isotropic) half-integer and integer quantum spin chains;[24] among other things, the latter always show an excitation gap, while the former are critical. The valence-bond-solid toy model (AKLT model)[25] in which each spin of length S is replaced by $2S$ fully symmetrized spin-1/2 objects on each site that are then linked up by singlet bonds between sites was found to explain all main features of integer quantum spin chains. One peculiarity of the AKLT model is that at each end of open spin chains S of the spin-1/2 objects find no singlet partner and form a free spin $S/2$ at each end. For integer spins as considered in the following, this leads in the AKLT model for *even* chain lengths to a $[2(S/2)+1]^2 = (S+1)^2$-fold degenerate ground state instead of the non-degenerate ground state found for periodic boundary conditions. The ground state of the magnetization $M = S + 1$ sector is then one of the (almost degenerate) lowest-lying bulk excitations combined with edge excitations. It is the interaction of the bulk and edge excitations which breaks the in principle exact degeneracy of the bulk excitation. This observation carries over to antiferromagnetic Heisenberg chains. There, one finds a group of $(S+1)^2$ low-lying states that become degenerate exponentially fast on the length scale of the bulk correlation length. The lowest-lying of these states has total spin 0 and magnetization 0; above this state there follows a spin-1 triplet, and so forth. The maximum total spin is given by S. The maximum magnetization is also given by S and concentrated at the edges. The lowest-lying excitation above them is the first true bulk excitation and corresponds to the lowest-lying state with $M = S + 1$. This phenomenon has been observed experimentally,[26] and generates a wealth of low-lying excitations if there are segments of spin chains of various length as is generically the case in the SCC's. For *odd* chain lengths, the situation is modified as the ground state has spin S instead of 0 and the lowest-lying states of the magnetization sectors $M \leq S$ are strictly degenerate both in the AKLT and Heisenberg models irrespective of the free-end-spin physics. The order of the low-lying (boundary) excitations is thus changed, but yet again, the ground state of the magnetization $S + 1$ sector contains the lowest-lying bulk excitation. This observation points to a special role of magnetization $M = S$, as will be seen throughout this paper.

In the present paper we focus on the ground-state properties of one-dimensional SCC's. We mostly consider *antiferromagnetic* coupling between the spins, which is probably the more common and also the more interesting situation compared to ferromagnetic coupling. To our knowledge, the exchange interaction in SCC's has not been studied previously, although exchange interactions between transition-metal ions in metal-organic complexes can be relatively large.[27,28,29,30] As we show

below, even the one-dimensional case with diamagnetic LS state, which is the simplest realistic case, shows quite rich behavior. In addition, the one-dimensional case allows to obtain essentially exact results.

II. THEORY

We start from the Hamiltonian

$$H_0 = -V \sum_{\langle ij \rangle} \sigma_i \sigma_j - B_0 \sum_i \sigma_i - h \sum_i S_i^z. \qquad (1)$$

The sum over $\langle ij \rangle$ counts all nearest-neighbor bonds once and the eigenvalues of S_i^z are $m_i = -S_i, -S_i + 1, \ldots, S_i$, where $S_i = S_{\mathrm{LS}}$ (S_{HS}) for $\sigma_i = 1$ (-1). V describes an interaction that for $V > 0$ ($V < 0$) favors homogeneous (alternating) arrangements of LS and HS. At least in a subset of known SCC's this interaction is of *elastic* origin.[31] Recently, Khomskii and Löw[15] have discussed this interaction more carefully, showing that it can be of *either* sign. We here approximate this interaction by a nearest-neighbor term. $2B_0 = \Delta > 0$ describes the energy difference between HS and LS and h is the physical magnetic field with g factor and Bohr magneton absorbed. The model so far is essentially equivalent to the one considered in Ref. 32. This model is integrable. The Hamiltonian H_0 is diagonal in the basis of simultaneous eigenstates of all $\mathbf{S}_i \cdot \mathbf{S}_i$ and S_i^z. In this basis

$$H_0 = -V \sum_{\langle ij \rangle} \sigma_i \sigma_j - B_0 \sum_i \sigma_i - h \sum_i m_i, \qquad (2)$$

where m_i is the quantum number of S_i^z.[33] For $h = 0$ we reobtain the Ising-type model introduced by Wajn-flasz and Pick[34] for magnetic molecular compounds and by Doniach[35] for lipidic chains. Here, each site can be in two states characterized by σ_i like in the Ising model, but the states are degenerate with degeneracies $2S_{\mathrm{LS}} + 1$ and $2S_{\mathrm{HS}} + 1$. It is known that the entropy change associated with the LS to HS transition is larger than predicted from these degeneracies.[5,32] This is attributed to the change in the vibrational properties between LS and HS states and can be approximately taken into account by effective degeneracy factors $G_{\mathrm{LS}}(T)$ and $G_{\mathrm{HS}}(T)$.[5,32] The model can be rigorously mapped onto an Ising model in a temperature-dependent effective field B.[35,36] This model has been treated in the mean-field approximation and with Monte Carlo simulations in two and three dimensions.[5] A related model for $\mathrm{TlSr_2CoO_5}$ with next-nearest-neighbor elastic interaction has recently been studied by Monte Carlo simulations in two dimensions and a number of stripe phases have been found.[15]

The physical magnetic field h was included by Garcia *et al.*[32] Their results can be obtained by a generalized mapping onto the standard Ising model. To our knowledge, the one-dimensional model suitable for triazole compounds has not been treated before.

We are interested in a model with an additional exchange interaction $J \neq 0$ between the magnetic ions. The Hamiltonian (1) is generalized to

$$H = H_0 - J \sum_{\langle ij \rangle} \mathbf{S}_i \cdot \mathbf{S}_j, \tag{3}$$

where $J > 0$ ($J < 0$) corresponds to a ferromagnetic (antiferromagnetic) coupling between the spins. The antiferromagnetic case appears to be more realistic since the interaction is due to superexchange.[37] To our knowledge, J has not been measured in SCC's, but it has been determined in very similar metal-organic complexes. It reaches $15\,\mathrm{K}$ and is indeed typically antiferromagnetic.[27,28,29] *Ab-initio* calculations find larger antiferromagnetic couplings, but are known to overestimate the exchange interaction.[30] On the other hand, in compounds based on Prussian blue, large *ferromagnetic* exchange interactions through CN^- ligands have been observed, leading to room-temperature ferromagnetism.[38] These experiments suggest that by suitable choice of ligands the interaction parameters V and J can be tuned to the same order of magnitude. It should also be noted that longer-range exchange interactions are exponentially suppressed and can be ignored. The dipole-dipole interaction is of long range in an isolated chain and might be the most important effect left out here. However, if the chain is deposited on a metallic surface, the dipole-dipole interaction becomes strongly screened.

The full Hamiltonian H still commutes with the operators $\mathbf{S}_i \cdot \mathbf{S}_i$. Thus the total spin *at each site* is still a constant of motion. On the other hand, H does no longer commute with S_i^z. In the case of Fe^{2+}, which is the most common magnetic ion in SCC's, we have $S_{\mathrm{HS}} = 2$ and $S_{\mathrm{LS}} = 0$ and a significant simplification occurs: For the nearest-neighbor interaction considered here any low spin partitions the chain into finite segments that do not interact *magnetically*. (Note that since $\mathbf{S}_i \cdot \mathbf{S}_i$ is a constant of motion, there are no eigenstates containing superpositions of LS and HS states.) Thus there is a close relation to the physics of finite spin chains. A low spin also interupts the propagation of spin waves. A spin-crossover chain could thus serve as a switchable *filter* for spin waves. In more than one dimension $S_{\mathrm{LS}} = 0$ leads to a less trivial percolation problem—for long-range order to be present it is necessary but not sufficient for the high spins to percolate.

In the following we restrict ourselves to $S_{\mathrm{LS}} = 0$. The Hamiltonian can be written as

$$\begin{aligned} H = {} & -V \sum_i (\sigma_i \sigma_{i+1} - 1) - B_0 \sum_i (\sigma_i - 1) \\ & - J \sum_i \mathbf{S}_i \cdot \mathbf{S}_{i+1} - h \sum_i S_i^z, \end{aligned} \tag{4}$$

where we have added a constant for convenience. Obviously, the energy of the pure LS state ($\sigma = +1$) vanishes.

The Ising-type operators σ_i all commute with the Hamiltonian H. Their eigenvalues ± 1 are thus good quantum numbers and the Hilbert space is a direct product of subspaces for given $\{\ldots, \sigma_i, \sigma_{i+1}, \ldots\}$.[33]

In each sector $\{\ldots, \sigma_i, \sigma_{i+1}, \ldots\}$ the system consists of chains of high spins separated by chains of low spins. The pure HS and LS states are obtained as the obvious limits. In Eq. (4) the LS chains do not contribute to the total energy, except for their ends. The total energy in a sector can thus be written as a sum over the energies of HS chains of various lengths, including a contribution from their ends. These HS chains do not interact magnetically since $S_{\mathrm{LS}} = 0$.

We are interested in the ground state and thus consider the *lowest* energy in each sector. The lowest energy in a sector can be written as the sum over the ground-state energies of non-interacting, finite HS chains. Note that H commutes with the total spin of each finite HS chain separately since these do not interact. The z-components M of the total spins of all the finite chains are thus also good quantum numbers. Let us denote the lowest energy of a HS chain of length n with magnetic quantum number M by $e_n^0(M)$, where $|M| \leq nS_{\mathrm{HS}}$. We write

$$e_n^0(M) = 4V + 2nB_0 - hM + \Delta e_n^0(M), \tag{5}$$

where the first term comes from the extra energy of the change from HS to LS at the ends. The final term is the lowest eigenenergy of the finite Heisenberg chain with open boundary conditions with the Hamiltonian $H_n = -J \sum_{i=1}^{n-1} \mathbf{S}_i \cdot \mathbf{S}_{i+1}$. Here, $S_i^2 = S_{\mathrm{HS}}(S_{\mathrm{HS}} + 1)$ for all $i = 1, \ldots, n$.

III. RESULTS AND DISCUSSION

For *ferromagnetic* coupling, $J > 0$, and magnetic field $h > 0$ both the exchange interaction and the Zeeman term prefer ferromagnetic alignment of spins. The lowest-energy state thus has the maximum magnetic quantum number $M = nS_{\mathrm{HS}}$ for each chain. The ground state of H_n for $J > 0$ is exactly the fully aligned state with energy $\Delta e_n^0(nS_{\mathrm{HS}}) = -(n-1)JS_{\mathrm{HS}}^2$. Thus for all $J \geq 0$:

$$e_n^0(nS_{\mathrm{HS}}) = 4V + 2nB_0 - nhS_{\mathrm{HS}} - (n-1)JS_{\mathrm{HS}}^2. \tag{6}$$

Now let us consider a sector $\{\ldots, \sigma_i, \sigma_{i+1}, \ldots\}$ for which the state consists of *volume fractions* p_n of HS chains of length n. The HS chains have to be separated by at least one low spin. When counting this low spin with each HS chain, the volume fractions become $(n+1)/n\, p_n$. Thus the volume fractions must satisfy the constraint

$$\sum_{n=1}^{\infty} \frac{n+1}{n} p_n \leq 1. \tag{7}$$

The energy per site is

$$\epsilon_0 = \sum_n p_n \frac{e_n^0(nS_{\mathrm{HS}})}{n}$$

$$= \sum_n p_n \left(\frac{4V + JS_{\mathrm{HS}}^2}{n} + 2B_0 - hS_{\mathrm{HS}} - JS_{\mathrm{HS}}^2 \right).\ (8)$$

We have to solve the linear optimization problem of minimizing ϵ_0 under the constraint (7). In the space of vectors $(p_1, p_2, \ldots)$ the region allowed by Eq. (7) is a hyperpyramid with apex at zero and the other corners at points with $p_m = m/(m+1)$ for one m and $p_n = 0$ for $n \neq m$. These are the points for which only chains of one single length are present and have the maximum volume fraction. This means that the finite HS chains are separated by *single* low spins. Since the allowed region is convex, the only possible solutions are its corners, except for special choices of parameters. Thus either $p_n = 0$ for all n (LS state) or $p_m = m/(m+1)$ for one m and all other $p_n = 0$. This strongly restricts the $\{\ldots, \sigma_i, \sigma_{i+1}, \ldots\}$ that can appear in any ground state. For the LS state, $\epsilon_0 = 0$, whereas for the state with nonzero p_n,

$$\epsilon_0 = \frac{4V - 2B_0 + 2JS_{\mathrm{HS}}^2 + hS_{\mathrm{HS}}}{n+1} + 2B_0 - hS_{\mathrm{HS}} - JS_{\mathrm{HS}}^2.$$
$$(9)$$

Examination shows that there are only three possible phases for $J \geq 0$: (i) If $4V - 2B_0 + 2JS_{\mathrm{HS}}^2 + hS_{\mathrm{HS}} > 0$ and $2B_0 - hS_{\mathrm{HS}} - JS_{\mathrm{HS}}^2 > 0$ or $4V - 2B_0 + 2JS_{\mathrm{HS}}^2 + hS_{\mathrm{HS}} < 0$ and $2V + B_0 - hS_{\mathrm{HS}}/2 > 0$ the ground state is the LS state. (ii) If $4V - 2B_0 + 2JS_{\mathrm{HS}}^2 + hS_{\mathrm{HS}} > 0$ and $2B_0 - hS_{\mathrm{HS}} - JS_{\mathrm{HS}}^2 < 0$ the ground state has $p_n > 0$ and all other $p_m = 0$, for $n \to \infty$, which corresponds to the HS state, and the energy is $\epsilon_0 = 2B_0 - hS_{\mathrm{HS}} - JS_{\mathrm{HS}}^2$. Note that the HS state appears for any values of V and h for sufficiently large exchange interaction J. This is similar to the exchange-induced Van-Vleck ferromagnetism in rare-earth compounds.[39] (iii) If $4V - 2B_0 + 2JS_{\mathrm{HS}}^2 + hS_{\mathrm{HS}} < 0$ and $2V + B_0 - hS_{\mathrm{HS}}/2 < 0$ the ground state has $p_1 = 1/2$ and all other $p_m = 0$. This corresponds to an *alternating* state of low and high spins. The energy is $\epsilon_0 = 2V + B_0 - hS_{\mathrm{HS}}/2$.

By using the LS/HS splitting B_0 as our unit of energy, we obtain a three-dimensional phase diagram in V/B_0, h/B_0, and J/B_0. The phase diagram is shown as the upper, $J \geq 0$, part of Fig. 8, below.

In the case of *antiferromagnetic* coupling, $J < 0$, there is a competition between the exchange and Zeeman terms in Eq. (4). Thus in principle finite HS chains of length n can occur with any magnetic quantum number M. The energy $e_n^0(M)$ of such a chain is given by Eq. (5). We introduce volume fractions $p_{n,M}$ of HS chains of length n with magnetic quantum number M. They must satisfy the constraint

$$\sum_{n=1}^\infty \sum_{M=-nS_{\mathrm{HS}}}^{nS_{\mathrm{HS}}} \frac{n+1}{n} p_{n,M} \leq 1. \qquad (10)$$

The energy per site is

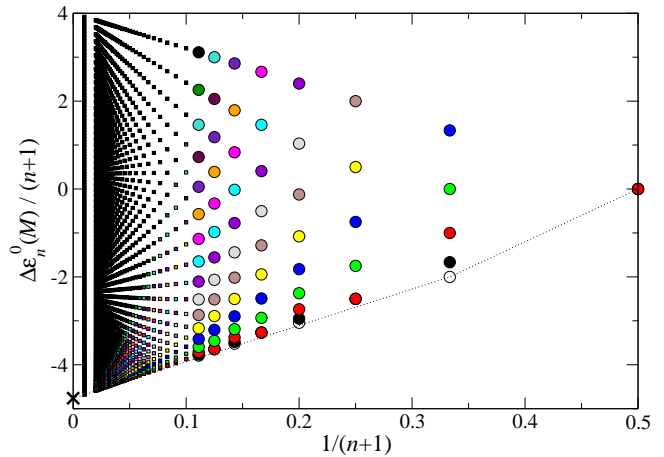$$\epsilon_0 = \sum_{n,M} p_{n,M} \left(\frac{4V - hM + \Delta e_n^0(M)}{n} + 2B_0 \right). \quad (11)$$

FIG. 1: (Color online). The lowest energies $\Delta e_n^0(M)/|J|$ of antiferromagnetic Heisenberg chains of length n for spin $S_{\mathrm{HS}} = 2$ in sectors with open boundary conditions for fixed total S^z quantum number M. The energies are normalized by a factor $1/(n+1)$ and shown as a function of $1/(n+1)$, where $n+1$ is the length of the chain counting one low spin per chain needed to separate HS chains. Circles: Results from exact Lanczos diagonalization. Squares: Results from DMRG, see text. Equal colors correspond to equal M. For odd n the energies for $M = 0$ (white), 1 (black), and 2 (red) are degenerate. The cross at $1/(n+1) = 0$ denotes the extrapolated energy density $-4.761248(1)$ of an infinite chain.[45]

Minimizing ϵ_0 under the constraint is again a linear optimization problem. Except for accidental degeneracies, the minima occur at the corners of the allowed parameter region. Thus either $p_{n,M} = 0$ for all n and M (LS state) or $p_{n,M} = n/(n+1)$ for one (n, M) and $p_{n,M} = 0$ for all others. Note that the period of the spin structure is then $n + 1$. In the latter case the energy per site is

$$\epsilon_0 = \frac{4V - 2B_0 - hM + \Delta e_n^0(M)}{n+1} + 2B_0. \qquad (12)$$

$\Delta e_n^0(M)/|J|$ is the lowest energy of the finite antiferromagnetic Heisenberg chain with open boundary conditions and the Hamiltonian $H_n' = \sum_{i=1}^{n-1} \mathbf{S}_i \cdot \mathbf{S}_{i+1}$ in the sector with total S^z quantum number M. It is not possible to find these energies in analytical form. For sufficiently small n, the Hamiltonian H_n' can be diagonalized numerically. However, the Hilbert space of H_n' has the dimension $(2S_{\mathrm{HS}} + 1)^n$, which quickly becomes intractable. We have calculated the energies up to $n = 8$ for all M using the Lanczos algorithm. The results for $\Delta e_n^0(M)/|J|/(n+1)$ are shown in Fig. 1 as colored circles, where identical colors denote the same values of M.

The energies for longer chains can be calculated with excellent precision with a finite-chain DMRG algorithm;[40,41] for a detailed explanation of the algorithm and its applications see Refs. 42,43. To obtain typically seven-digit precision for the ground state energy per site, we have kept up to $M = 300$ states in the reduced DMRG Hilbert spaces and carried out three finite-system sweeps

which was enough to ensure convergence. Note that DMRG prefers open to periodic boundary conditions; in the present application, this matches the physical situation. In standard DMRG applications to integer-spin chains, end spins of length $S/2$ (i.e., a spin 1 at each end for our case) are attached to eliminate the peculiar boundary degrees of freedom and access bulk physics directly.[40,44] In the present calculation, these boundary degrees of freedom are physical and hence no end spins are attached.

The energies for lengths $n = 9$ through $n = 49$ as well as $n = 99$ (to mimic the pure HS phase) are shown in Fig. 1 by squares. (For $M = nS_{\mathrm{HS}} - 2$ and $M = nS_{\mathrm{HS}} - 1$ the results have been obtained by exact numerical diagonalization. For $M = nS_{\mathrm{HS}}$ the exact analytical value $\Delta e_n^0(nS_{\mathrm{HS}})/|J| = (n-1)S_{\mathrm{HS}}^2$ has been used.)

We first consider the case of vanishing magnetic field, $h = 0$. Figure 1 shows that the state with $M = 0$ has the lowest energy for any n. Then $\epsilon_0 = (4V - 2B_0 + \Delta e_n^0(0))/(n+1) + 2B_0$ is a sum of $\Delta e_n^0(0)/(n+1)$ and a *linear* function in $1/(n+1)$. The minimum of ϵ_0 can only occur for $n = 1$, $n = 2$, or $n \to \infty$, since all other points lie above the dotted straight lines connecting the corresponding points in Fig. 1 (not obvious on this scale). The relevant energies per site are thus determined by $\Delta e_1^0/2 = 0$, $\Delta e_2^0/3 = 2J$, and $\lim_{n\to\infty} \Delta e_n^0/(n+1) = 4.761248\,J$ and have to be compared to the LS energy $\epsilon_0 = 0$. The resulting phase diagram is shown in Fig. 2. Note the appearance of a *dimer* phase with $n = 2$. In this phase the energy increase due to the HS-HS pairs ($V < 0$ prefers HS-LS neighbors) is overcompensated by the energy decrease due to the formation of spin singlets. Thus this phase is stabilized by the large negative singlet formation energy of Heisenberg spin pairs. Figure 1 shows that a similar energy decrease is also found for the other even chain lengths $n = 4, 6, \ldots$ but that it is not large enough to stabilize these states as the ground state.

For general magnetic field h we have to take all possible magnetic quantum numbers M of the chains into account. This is obviously impossible for the pure HS phase. Instead, we have performed DMRG calculations for chain length $n = 99$ for all possible magnetizations $M = 0, \ldots, 198$ and use them as a caricature of the HS state. Since in the $n = 99$ state one spin in 100 is in the LS state, we expect quantitative errors of the order of 1%. We check the errors quantitatively below.

The parameter space is again effectively three-dimensional since we take B_0 as our unit of energy. For each set of parameters (V, J, h) we calculate the minimum energy densities for all states with $n \leq 49$ as well as $n = 99$ from Eq. (12). The energy density of the LS state is zero. Then the ground state is obtained by finding the minimum energy. Figure 3 shows a series of phase diagrams in (V, h) space for fixed exchange interaction J. Note that the lower edges of each diagram, i.e., $h = 0$, are consistent with Fig. 2. We observe that the dimer ($n = 2$) phase present at $h = 0$ is suppressed by the field,
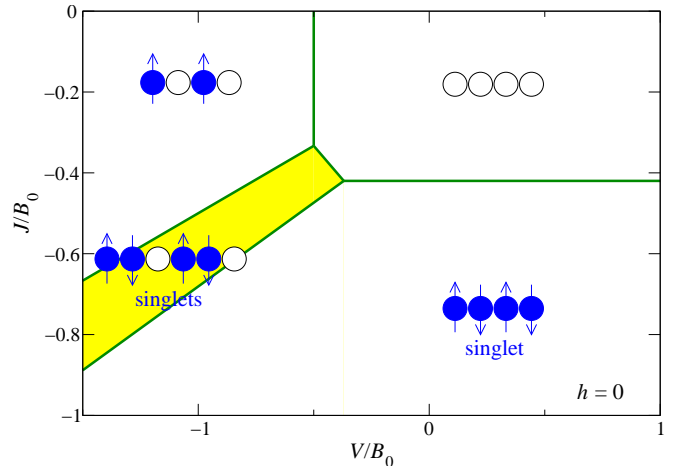

FIG. 2: (Color online). Ground-state phase diagram of the 1D spin-crossover model with $S_{\mathrm{LS}} = 0$ and $S_{\mathrm{HS}} = 2$ for vanishing magnetic field, $h = 0$, and antiferromagnetic exchange interaction, $J < 0$. The dimer ($n = 2$) phase case is highlighted. The heavy solid lines denote discontinuous transitions. The various spin structures are indicated by cartoons (solid symbols: HS state, open symbols: LS state); these should not be overinterpreted—there is no long-range order.

as is expected since this phase is stabilized by the singlet formation energy.

The phase boundaries involving the HS state (black) are markedly curved, although the energy of each phase is a *linear* function of the parameters V, B_0, J, h so that the phase boundaries should be straight. The explanation is that the HS phase does not have constant magnetization in the ground state. For *optimized* magnetization, the ground-state energy in the HS sector is not linear in the parameters. We come back to the ground-state magnetization below.

For $J \lesssim -0.6$ the phase diagrams remain qualitatively the same. The features are shifted to lower V and expanded linearly in both the V and h directions. Letting V, J, and h go to infinity while keeping their ratios fixed corresponds to the limit $B_0 \to 0$, i.e., vanishing energy difference between LS and HS states. In this limit we choose $|J|$ as our unit of energy, leaving two dimensionless parameters $V/|J|$ and $h/|J|$. The resulting phase diagram is shown in Fig. 4.

Interesting behavior is seen in the triangular region surrounded by phases with $n = 1$, $n = 2$, and the HS phase, as shown in Fig. 4(b). Here, phases with HS chain lengths $n = 3$, 5, 7, and 9 are found. We do not observe any further phases. To understand why only *odd* chain length n appear, we refer to the energy densities in Fig. 1: For even n, the energy of the singlet ($M = 0$) state is *lower* than expected from a linear fit, at least for the small n relevant here, while for odd n it is higher (note the white circles). Thus at zero magnetic field, even-n states are preferred. As discussed above, only $n = 2$ actually appears as a ground state. On the other hand, for even n, the energy of states with $M \geq 2$ is *higher*
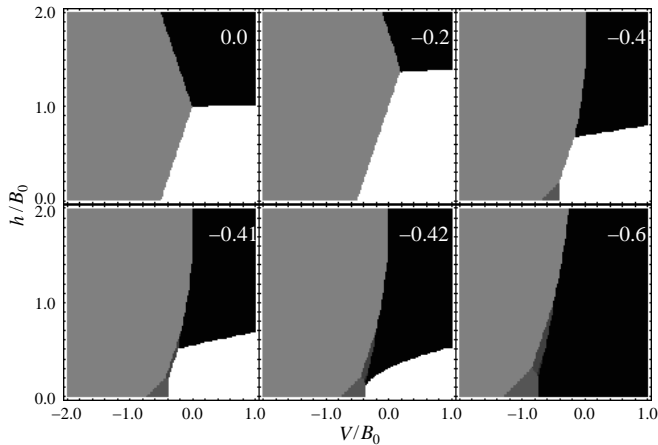
FIG. 3: Zero-temperature phase diagrams for the same model as in Fig. 2, but in a magnetic field, for antiferromagnetic exchange interactions $J/B_0 = 0.0$, -0.2, -0.4, -0.41, -0.42, -0.6. The white area corresponds to the LS phase, the black to the HS phase, approximated by a phase with $n = 99$, and the gray areas correspond to $n = 1, 2, 3, 5$ (from light to dark). All transition are discontinuous, the purely magnetic continuous transition discussed below is not shown.
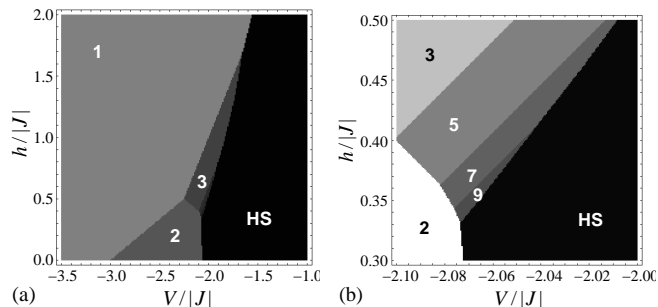

FIG. 4: (a) Zero-temperature phase diagrams as in Fig. 3 in the limit $B_0 \to 0$ (or $V, J, h \to \infty$ with their ratios fixed). The gray scale is the same as in Fig. 3. (b) Enlargement of the left figure on a *different gray scale*. The values of n in the various ground states are indicated.

than a linear fit, while for odd n it is lower (note, for example, the red circles). Thus in a sufficiently large magnetic field odd-n states are preferred. The fact that the series of odd n is cut off at $n = 9$ is a result of the detailed numerical values of energies in Fig. 1—for larger n, the HS state happens to have the lower energy. While we expect the appearance of only odd HS chain lengths to be a robust feature of spin-crossover chains with strong antiferromagnetic interaction, the restriction to $n \le 9$ should thus be model dependent. For example, inclusion of a next-nearest-neighbor elastic interaction or a different integer value of S_{HS} may change this result.

We next turn to the magnetic properties of the various ground states. Figure 5 shows the magnetic quantum number M of the finite HS chains and the magnetization m in the ground states in the limit of large V, J, h. The magnetization is defined as the magnetic quantum
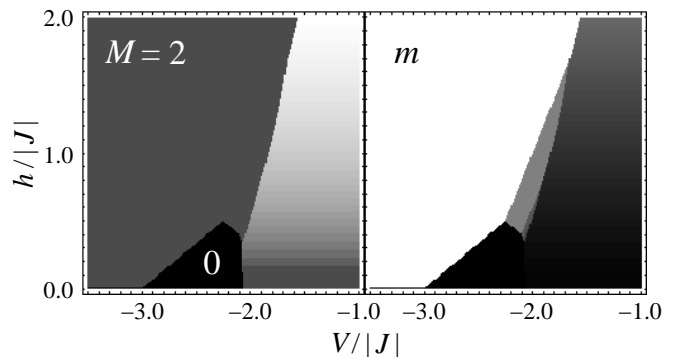

FIG. 5: Left: Density plot of the magnetic quantum number M of the finite chains in the same parameter region as in Fig. 4(a). Black corresponds to $M = 0$, white to maximum M. The phases with odd n all have $M = 2$. Right: Magnetization $m = M/(n + 1)$ derived from the data in the left plot. Black (white) corresponds to $m = 0$ ($m = 1$). The magnetization of the fully polarized HS state, which does not appear in the plot, would be $m = S_{HS} = 2$.

number M per site, taking the separating low spins into account, i.e.,

$$m = \frac{M}{n + 1}. \tag{13}$$

Interestingly, the phases with odd n all have $M = S_{HS} = 2$, including the $n = 7$ and $n = 9$ phases not resolved in Fig. 5. This of course corresponds to different *magnetizations* m, as shown in the right-hand plot in Fig. 5. To understand the special significance of the value $M = S_{HS} = 2$, we plot in Fig. 6 the local expectation values of the spins, $\langle S_i^z \rangle$, for each site of a HS chain of length $n = 9$, obtained with DMRG. The plot shows that for $0 < M \le S_{HS}$ the chain can accomodate the finite spin by forming a Néel-type state. (For an Ising chain, the state with $M = S_{HS}$ is clearly realized by $\langle S_i^z \rangle = (-1)^{i+1} S_{HS}$.) For higher M this is no longer possible and spins pointing in the "wrong" direction are reduced (a bulk magnon is excited), as seen in Fig. 6. This costs exchange energy and it turns out that such states are always higher in energy than competing phases.

The dimer ($n = 2$) phase always consists of two-high-spin singlets, $M = 0$. This shows that it is energetically favorable to replace the dimer state by a state with odd n or the HS state, instead of having $M > 0$ for the dimers.

Finally, we turn to the pure HS phase. At $T = 0$ the system is equivalent to an infinite antiferromagnetic $S = S_{HS}$ chain. We thus expect the magnetization to rise continuously with increasing magnetic field h and to reach its maximum value $m = S_{HS}$, i.e., full spin alignment, at a *continuous* phase transition. Since we approximate the HS phase by the $n = 99$ phase, the continuous increase is replaced by small steps in Fig. 5. The position of this transition is determined by equating the energies per site for $M = nS_{HS}$ and $M = nS_{HS} - 1$. From Eq. (12)
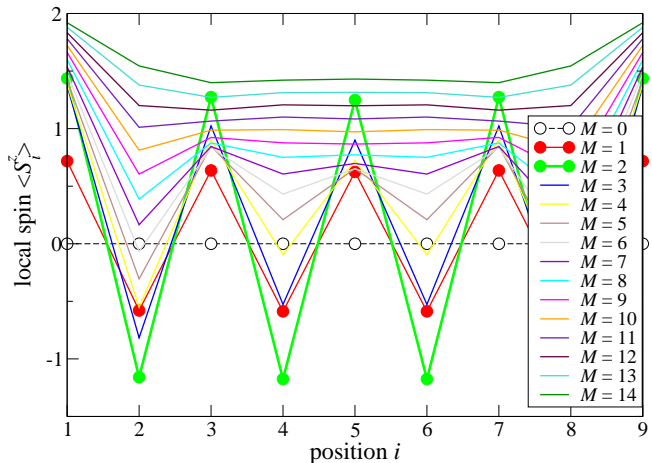
FIG. 6: (Color online). Local expectation values $\langle S_i^z \rangle$ for each site of a HS chain of length $n = 9$ for various total magnetic quantum numbers of the chain, M. The values have been obtained by DMRG.

FIG. 7: (Color online). Expectation value of the z-component of the spins, $\langle S^z \rangle$, and spin-spin correlation functions at the separation of $|i - j| = 4$ as functions of the total magnetic quantum number M. Inset: Correlation function $\langle S_i^+ S_j^- \rangle$ as a function of separation for three values of the total magnetic quantum number M.

we thus obtain the critical field

$$h_c = \Delta e_n^0(2n) - \Delta e_n^0(2n - 1), \tag{14}$$

which is proportional to J and independent of B_0 and V. For $n = 99$ exact diagonalization yields $h_c \approx -7.9980\,J$. This can be compared with the exact result for an infinite chain, which is easily found to be $h_c = -4JS_{\mathrm{HS}} = -8\,J$. Thus our result for $n = 99$ is already very close. This also gives an indication of the order of magnitude of errors. By restricting the DMRG calculations to $n < 100$ we make an error for the transition to full spin alignment of the order of 0.03%. As another way to estimate the errors, we determined the triple point between LS, HS, and dimer ($n = 2$) phases in zero field and compared the result to the "exact" triple point shown in Fig. 2. The error is of the order of 0.2% for V and 0.1% for J, indistinguishable on the scale of the figure.

It is obvious to ask about the critical behavior close to this continuous transition. We define the deviation of the magnetization from its maximum by $\Delta m \equiv S_{\mathrm{HS}} - m$. Plotting Δm^2 vs. h close to h_c (not shown) we find that, apart from steps originating from the finite $n = 99$, Δm^2 is linear in $h_c - h$ so that the critical exponent of Δm with respect to the field h is mean-field-like, $\beta = 1/2$.

We also obtain spin correlations from the DMRG. Figure 7 shows spin-spin correlation functions for $n = 99$ for two spins close to the center of the chain, where the infinite chain should be well approximated. We first notice the anomaly at $M = 2$. This is of the same origin as the stabilization of $M = 2$ for small odd chain lengths, discussed above. It is thus a finite-size effect not present for the true HS phase. Apart from this anomaly, the *transverse* correlations $\langle S_i^+ S_j^- \rangle$ first grow with magnetic field h or magnetization. This is the one-dimensional analog of the spin-flop state in ordered antiferromagnets, where the staggered magnetization is oriented perpendicularly
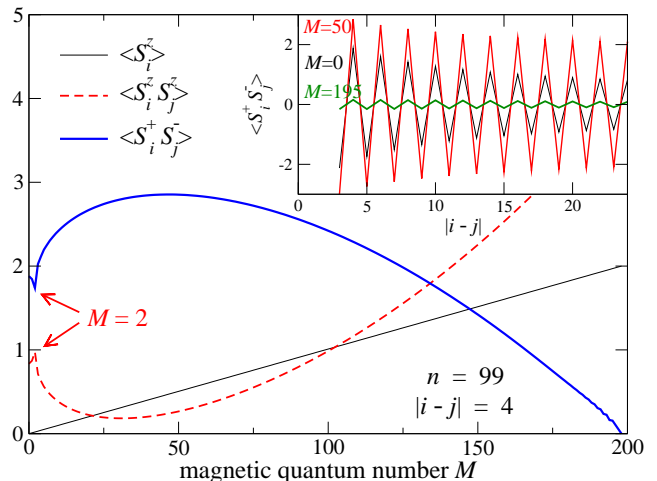
to the applied field. For large fields, the correlations decrease again since the spins are more and more forced into the field direction. In the fully polarized state for $h \geq h_c$ the transverse fluctuations vanish.

As a summary, we show in Fig. 8 the three-dimensional phase diagram. The continuous transition to full spin alignment is indicated by the heavy solid outline. All other surfaces are discontinuous transitions between states with different chain length n. Horizontal cuts correspond to the plots in Fig. 3. The vertical cut at $h = 0$ corresponds to Fig. 2.

To conclude, we have studied a model for spin-crossover compounds forming one-dimensional chains. We consider spin quantum numbers appropriate for Fe^{2+} ions, which have a spin-0 LS and a spin-2 HS state. The model includes elastic and exchange interactions and an external magnetic field. We obtain the ground-state phase diagram analytically for ferromagnetic or zero exchange interaction and using the density-matrix renormalization group (DMRG) for antiferromagnetic exchange. Besides a diamagnetic LS phase and a HS phase equivalent to the usual Heisenberg chain we find a number of more complex phases. For sufficiently negative elastic interaction V we find an alternating phase of low and high spins. In bulk, three-dimensional SCC's the corresponding checkerboard state with low and high spins forming nearest neighbors has been observed experimentally.[13]

For antiferromagnetic coupling, which is the more realistic and more interesting case, we find a robust dimer ($n = 2$) phase, which consists of spin singlets ($M = 0$) formed by two high spins separated by single low spins. This phase is stabilized by the relatively large energy reduction due to singlet formation of two spins and
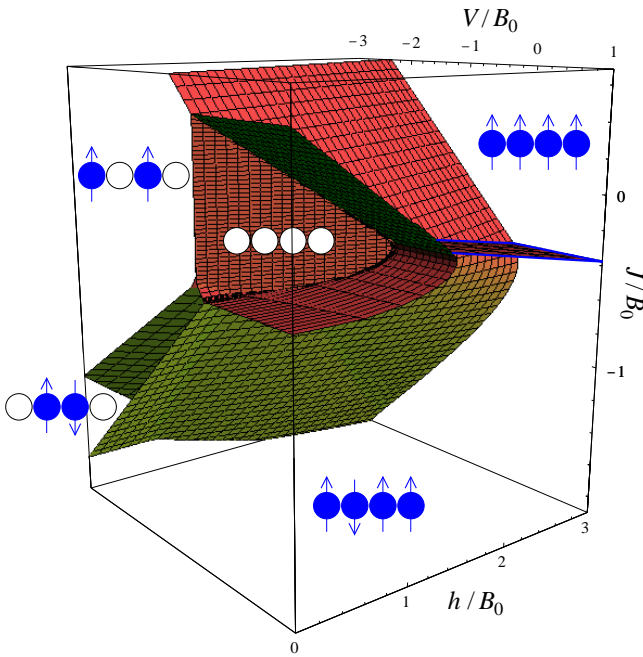
FIG. 8: (Color online). Zero-temperature phase diagram of the spin-crossover chain with $S_{LS} = 0$ and $S_{HS} = 2$. Positive (negative) J/B_0 corresponds to ferromagnetic (antiferromagnetic) exchange interaction. The solid surfaces denote phase transitions between different phases, which are indicated. The phases with HS chain lengths $n = 3, 5, \ldots$ are hidden in this view. All transitions are discontinuous, except for the continuous transition to full spin alignment in the HS phase, marked by the solid blue outline.

would thus be absent for an Ising exchange interaction, $-J \sum_i S_i^z S_{i+1}^z$. Since this phase appears at zero and low magnetic fields, it should be accessible experimentally. As the magnetic field is increased, the dimers remain in the singlet state until states with an odd number of HS ions or the pure HS state become lower in energy, whereupon the singlet dimer phase is destroyed in a discontinuous transition.

At higher magnetic fields we find a number of phases consisting of finite chains of length $n = 3, 5, 7, 9$ of ions in the high-spin state with total S^z quantum number $M = 2$ separated by single ions in the diamagnetic low-spin state. We argue that the succession of odd chain lengths is a robust feature, while the restriction to just these odd numbers is not.

We find that a model that contains the most important ingredients of one-dimensional spin-crossover chain molecules shows a rich ground-state phase diagram. The model is related to various systems studied in recent years, such as site-diluted spin models and finite antiferromagnetic Heisenberg chains. Obvious questions for the future concern the behavior at nonzero temperature and of higher-dimensional models, in which *percolation* plays an important role if the LS state is diamagnetic. New physics beyond that of diluted spin models comes into play since the dilution by LS ions is not quenched disorder but a dynamical degree of freedom.

[*] Electronic address: timm@physik.fu-berlin.de

[1] C. Joachim, J. K. Glimzewski, and A. Aviram, Nature **408**, 541 (2000).

[2] A. Nitzan and M. A. Ratner, Science **300**, 1384 (2003).

[3] J. Zarembowitch and O. Kahn, New J. Chem. **15**, 181 (1991); O. Kahn, J. Krber, and C. Jay, Advan. Mater. **4**, 718 (1992).

[4] O. Kahn and C. Jay Martinez, Science **279**, 44 (1998).

[5] H. Bolvin and O. Kahn, Chem. Phys. **192**, 295 (1995); Chem. Phys. Lett. **243**, 355 (1995).

[6] L. Cambi and L. Szegö, Ber. Dtsch. Chem. Ges. **64**, 259 (1931); **66**, 656 (1933).

[7] P. Gütlich, Struct. Bonding (Berlin) **44**, 83 (1981).

[8] E. König, Struct. Bonding (Berlin) **76**, 51 (1991).

[9] P. Gütlich, Y. Garcia, and H. A. Goodwin, Chem. Soc. Rev. **29**, 419 (2000).

[10] S. J. Blundell and F. L. Pratt, J. Phys.: Condens. Matter **16**, R771 (2004).

[11] S. Decurtins, P. Gütlich, C. P. Köhler, H. Spiering, and A. Hauser, Chem. Phys. Lett. **105**, 1 (1984); S. Decurtins, P. Gütlich, K. M. Hasselbach, H. Spiering, and A. Hauser, Inorg. Chem. **24**, 2174 (1985).

[12] W. Fujita and K. Awaga, Science **286**, 261 (1999); M. E. Itkis, X. Chi, A. W. Cordes, and R. C. Haddon, Science **296**, 1443 (2002).

[13] M. Coutanceau, P. Dordor, J.-P. Doumerc, J.-C. Grenier, P. Maestro, M. Pouchard, D. Sedmidubsky, and T. Seguelong, Solid State Commun. **96**, 569 (1995); J.-P. Doumerc, J.-C. Grenier, P. Hagenmuller, M. Pouchard, and A. Villesuzanne, J. Solid State Chem. **147**, 211 (1999); J.-P. Doumerc, M. Coutanceau, A. Demourgues, E. Elkaim, J.-C. Grenier, and M. Pouchard, J. Mater. Chem. **11**, 78 (2001).

[14] T. Yokoyama, Y. Murakami, M. Kiguchi, T. Komatsu, and N. Kojima, Phys. Rev. B **58**, 14238 (1998).

[15] D. I. Khomskii and U. Löw, Phys. Rev. B **69**, 184401 (2004).

[16] A. Grohmann (private communication).

[17] *Carbon Nanotubes, Topics in Applied Physics*, vol. **80**, edited by M. S. Dresselhaus, G. Dresselhaus, and P. Avouris (Springer, Berlin, 2001).

[18] R. G. Endres, D. L. Cox, and R. R. P. Singh, Rev. Mod. Phys. **76**, 195 (2004).

[19] O. P. Vajk, P. K. Mang, M. Greven, P. M. Gehring, and

J. W. Lynn, Science **295**, 1691 (2002).

[20] K. Kato, S. Todo, K. Harada, N. Kawashima, S. Miyashita, and H. Takayama, Phys. Rev. Lett. **84**, 4204 (2000); A. W. Sandvik, Phys. Rev. Lett. **86**, 3209 (2001); A. W. Sandvik, Phys. Rev. B **66**, 024418 (2002).

[21] R. Yu, T. Roscilde, and S. Haas, cond-mat/0410041 (unpublished).

[22] W. Selke, V. L. Pokrovsky, B. Büchner, and T. Kroll, Eur. Phys. J. B **30**, 83 (2002); R. Leidl and W. Selke, Phys. Rev. B (in press), cond-mat/0404555; M Holtschneider, R. Leidl, and W. Selke, cond-mat/0406403 (unpublished).

[23] A. Imambekov, M. Lukin, and E. Demler, Phys. Rev. A **68**, 063602 (2003); Phys. Rev. Lett. **93**, 120405 (2004).

[24] F. D. M. Haldane, Phys. Rev. Lett. **50**, 1153 (1983).

[25] I. Affleck, T. Kennedy, E. H. Lieb, and H. Tasaki, Phys. Rev. Lett. **59**, 799 (1987).

[26] M. Hagiwara, K. Katsumata, I. Affleck, B.I. Halperin, J.P. Renard, Phys. Rev. Lett. **65**, 3181 (1990).

[27] O. Waldmann, J. Hassmann, P. Müller, G. S. Hanan, D. Volkmer, U. S. Schubert, and J.-M. Lehn, Phys. Rev. Lett. **78**, 3390 (1997).

[28] C. Boskovic, A. Sieber, G. Chaboussant, H. U. Güdel, J. Ensling, W. Wernsdorfer, A. Neels, G. Labat, H. Stoeckli-Evans, and S. Janssen, Inorg. Chem. **43**, 5053 (2004).

[29] T. Lancaster, S. J. Blundell, F. L. Pratt, M. L. Brooks, J. L. Manson, E. K. Brechin, C. Cadiou, D. Low, E. J. L. McInnes, and R. E. P. Winpenny, J. Phys.: Condens. Matter **16**, S4563 (2004).

[30] A. V. Postnikov, G. Bihlmayer, and S. Blügel, cond-mat/0409302 (unpublished).

[31] N. Willenbacher and H. Spiering, J. Phys. C **21**, 1423 (1988); J. Phys.: Condens. Matter **1**, 10089 (1989).

[32] Y. Garcia, O. Kahn, J.-P. Ader, A. Buzdin, Y. Meurdesoif, and M. Guillot, Phys. Lett. A **271**, 145 (2000).

[33] Here, σ_i is a quantum number, not an operator, but it is permissable to use the same symbol since the operator σ_i commutes with any other operator.

[34] J. Wajnflasz, J. Phys. Status Solidi **40**, 537 (1970); J. Wajnflasz and R. Pick, J. Phys. (Paris), Colloq. **32**, C1 (1971).

[35] S. Doniach, J. Chem. Phys. **68**, 4912 (1978).

[36] M. Nielsen, L. Miao, J. H. Ipsen, O. G. Mouritsen, and M. J. Zuckermann, Phys. Rev. E **54**, 6889 (1996).

[37] P. W. Anderson, Phys. Rev. **79**, 350 (1950).

[38] S. Ferlay, T. Mallah, R. Ouahès, P. Veillet, and M. Verdaguer, Nature **378**, 701 (1995).

[39] P. Fulde and I. Peschel, Adv. Phys. **21**, 1 (1972).

[40] S.R. White, Phys. Rev. Lett. **69**, 2863 (1992).

[41] S.R. White, Phys. Rev. B **48**, 10345 (1993).

[42] I. Peschel, X. Wang, K. Hallberg, M. Kaulke (eds.): *Density Matrix Renormalization*, Springer (1999).

[43] U. Schollwöck, Rev. Mod. Phys. (in press), cond-mat/0409292.

[44] U. Schollwöck and T. Jolicœur, Europhys. Lett. **30**, 493 (1995).

[45] U. Schollwöck, O. Golinelli, and T. Jolicœur, Phys. Rev. B **54**, 4038 (1996).